Polymer 51 (2010) 3031–3038

Contents lists available at ScienceDirect

Polymer

journal homepage: www.elsevier.com/locate/polymer

Tailoring side chains of low band gap polymers for high efficiency polymer solar cells

Weiwei Li [a,b], Ruiping Qin [c], Yi Zhou [b], Mattias Andersson [b], Fenghong Li [b], Chi Zhang [a], Binsong Li [a], Zhengping Liu [c], Zhishan Bo [a,*], Fengling Zhang [b,**]

[a] Beijing National Laboratory for Molecular Sciences, Institute of Chemistry, Chinese Academy of Sciences, Beijing 100190, China
[b] Department of Physics, Chemistry and Biology, Linköping University, SE-58183 Linköping, Sweden
[c] College of Chemistry, Beijing Normal University, Beijing 100875, China

ARTICLE INFO

Article history:
Received 17 February 2010
Received in revised form
22 April 2010
Accepted 9 May 2010
Available online 15 May 2010

Keywords:
Organic solar cell
Side chains
Low band gap

ABSTRACT

High efficiency organic solar cells (OSCs) require conjugated polymers with a low band gap, broad absorption in visible and IR region, high carrier mobility, and relatively high molecular weight as p-type donor materials. Flexible side chains on the rigid polymer backbone are crucial for the solubility of conjugated polymers. In this work, four polymers with the main chain structure of fluorene-thiophene-benzothiadiazole-thiophene and flexible side chains located on fluorene, thiophene, and benzothiadiazole moiety, respectively, have been synthesized by Suzuki–Miyaura–Schlüter polycondensation. Photovoltaic device measurements with a device configuration of ITO/polymer:$PC_{71}BM$ blends/LiF/Al show that **P1** carrying octyloxy chains on benzothiadiazole rings gives the best performance, with a power conversion efficiency of 3.1%.

1. Introduction

In the past two decades, plastic solar cells as an alternative to inorganic photovoltaic devices have been investigated due to their flexibility and low cost of processing [1,2]. Organic solar cells (OSC) based on regioregular poly(3-hexylthiophene) (P3HT) donor and a soluble fullerene derivative acceptor, with a bulk heterojunction structure, have reached power conversion efficiencies (PCE) of 5% [3,4]. Until now, more and more conjugated polymers have been developed and used for OSCs. Benefiting from their low band gap, broad absorption in the visible and infrared (IR) region, crystallization, and/or high carrier mobility, PCEs of 5%–7.5% have been achieved [5–11].

Several groups have devoted to designing new optimized conjugated polymers, improving efficiency, and decreasing the cost of processing for device fabrication [12–14]. Low band gap conjugated polymers with main chain alternating donor–acceptor (D–A) structure are promising, which can broaden the absorption to the red and even to the near IR region via the so-called internal charge transfer and result in higher PCE [15]. Functional groups such as fluorene [16–20], carbazole [6,9,21,22], silafluorene [7,23], cyclopentadithiophene [8,24–26], *N*-substituted dithienopyrrole [27,28] and dithienosilole [10,29], have been used as donor moieties; whereas, functional groups such as benzothiadiazole [12,30], quinoxaline [26,31,32], diketopyrrolopyrrole [33,34], thienopyrazine [35,36], fluoranthene [37] and so on were usually used as acceptor moieties.

The rigid conjugated polymers are usually required to carry flexible side chains to ensure that polymers have certain solubility in organic solvents. The lengths of alkyl chains play an important role in molecular weights, energy levels of conjugated polymers, morphologies of blend films, and therefore the photovoltaic performance of devices [19,38,39]. Moreover, the position of alkyl chain on each D–A repeat unit is also a key point in tailoring polymer structures [9,35,40–43]. Our previous work about a copolymer named poly(2-(5-(5,6-bis(octyloxy)-4-(thiophen-2-yl) benzo[c][1,2,5]thiadiazole-7-yl) thiophene-2-yl)-9-octyl-9H-carbazole) (**HXS-1**), with two octyloxy chains on benzothiadiazole moiety demonstrated that a planar structure was formed due to the low steric hinderance of octyloxy chain, and a PCE of 5.4% was achieved [9]. Janssen et al. have synthesized a series of conjugated polymers based on the thiophene-benzothiadiazole-thiophene structure, among which the polymer with octyl substituents on the 3-position of thiophene bears much more steric hinderance than that with octyl substituents on the 4-position of thiophene, and results in different optical and electrochemical properties for these two polymers [41,42].

* Corresponding author. Tel./fax: +86 10 82618587.
** Corresponding author. Tel.: +46 13281257; fax: +46 13288969.
E-mail addresses: zsbo@iccas.ac.cn (Z. Bo), fenzh@ifm.liu.se (F. Zhang).

0032-3861/$ – see front matter © 2010 Elsevier Ltd. All rights reserved.
doi:10.1016/j.polymer.2010.05.015

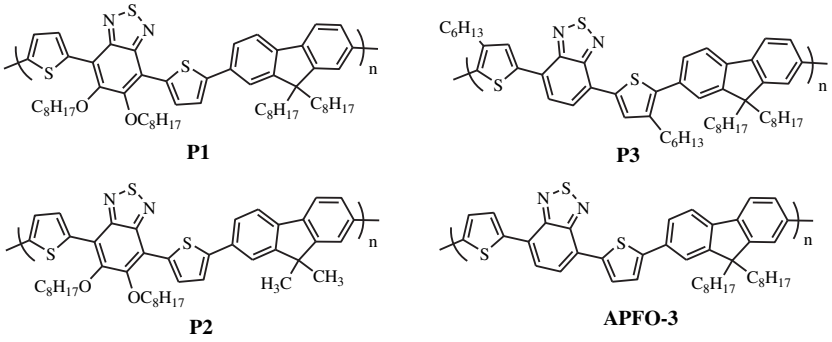

Chart 1. The chemical structures of low band gap polymers.

In this work, three conjugated polymers **P1**–**3** with the structure fluorene-thiophene-benzothiadiazole-thiophene have been synthesized via Suzuki- Miyaura-Schlüter polycondensation (SMSPC), in which the flexible chains are placed on the fluorene, thiophene or benzothiadiazole units, as shown in Chart 1. A similar polymer, poly(2,7-(9,9-dioctyl-fluorene)-*alt*-5,5-(4,7-di-2-thienyl-2,1,3-benzothiadiazole (**APFO-3**) [39], is also listed for comparison. High molecular weight and good solubility are essential for polymers used to fabricate photovoltaic devices via solution process. [44–48] In previous work, for **APFO-3** only low molecular weight material can be achieved due to its poor solubility. When octyl side chains were replaced by dodecyl side chains, the number molecular weight (M_n) can be increased to 12 kg/mol, however, PCE decreased from 2.1% for **APFO-3** to 1.4% for dodecyl-substituted polymer. [39] In our work, polymer **P1** with octyloxy chains on the benzothiadiazole has a M_n of 77.1 kg/mol and a weight average molecular weight (M_w) of 130.5 kg/mol, which is higher compared to the relatively low molecular weight of **APFO-3** with $M_n = 6.2$ kg/mol and $M_w = 14$ kg/mol. Polymer **P3** with hexyl chains on the thiophene units gave the highest molecular weight with $M_n = 175$ kg/mol and $M_w = 318$ kg/mol. Photovoltaic devices based on polymer/$PC_{71}BM$ blends were fabricated by spin-coating from two different solutions: chloroform or dichlorobenzene (DCB). Devices based on polymer **P1** and **P2** with octyloxy substituents on the benzothiadiazole reach high performances with PCE 3.1% for **P1**/$PC_{71}BM$ from DCB solution and 2.8% for **P2**/$PC_{71}BM$ from chloroform solution. Their PCEs are comparable with that of **APFO-3**, which gives high PCE 2.7% from DCB solution. **P3** gives the lowest PCE of 2.2% among these polymers, possibly due to the steric hinderance of the hexyl substituents on the thiophene moieties. Our studies have shown that flexible side chains have great influence on the photovoltaic properties of conjugated polymers. Moreover, current-voltage characteristics of devices, and morphologies and mobilities of blend films depend strongly on the solvent used for spin-coating.

2. Experimental section

2.1. Materials and instruments

All chemicals were purchased from commercial suppliers and used without further purification. THF and Et_2O were distilled from sodium with benzophenone as an indicator under nitrogen atmosphere. Hexane and CH_2Cl_2 were distilled from CaH_2. Chloroform was distilled before use. 4,7-bis(5-bromothiophen-2-yl)-5,6-bis (octyloxy)- 2,1,3-benzothiadiazole (**4**) [9], 4,4,5,5-tetramethyl-2-(2-(4,4,5,5-tetramethyl-1,3,2- dioxaborolan-2-yl)-9,9-dioctyl-9H-fluoren-7-yl)-1,3,2-dioxaborolane (**5**) [16], 4,4,5,5-tetramethyl -2-(9,9-dimethyl-2-(4,4,5,5-tetramethyl-1,3,2-dioxaborolan-2-yl)-9H-fluoren-7-yl)-1,3,2-dioxaborolane (**6**) [49], 4,7-bis(5-bromo-4-hexylthiophen-2-yl)-2,1,3- benzothiadiazole (**7**) [41], and $Pd(PPh_3)_4$ [50] were prepared according to literature procedures. All reactions were performed under an atmosphere of nitrogen and monitored by thin layer chromatography (TLC) on silica gel 60 F254 (Merck, 0.2 mm). Column chromatography was carried out on silica gel (200–300 mesh).

^1H and ^{13}C NMR spectra were recorded on a Bruker DM 300 or AV 400 spectrometer in $CDCl_3$. Gel permeation chromatography (GPC) measurements were performed on a Waters chromatography

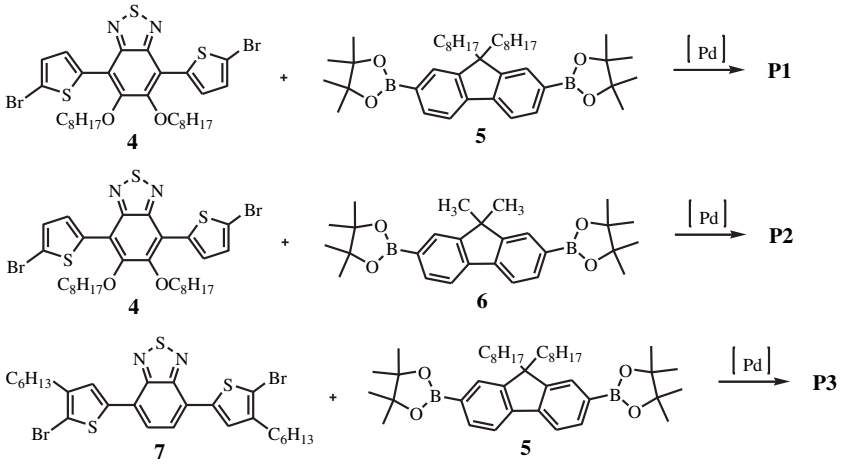

Scheme 1. The synthesis route of polymers **P1**–**3.**

Table 1
Number average molecular weight (M_n), weight average molecular weight (M_w), polydispersity index (PDI), glass transition temperature (T_g) and degradation temperature (T_d) of **P1**–**3** and **APFO-3**.

polymer	M_n [kg/mol]	M_w [kg/mol]	PDI	T_g [°C]	T_d [°C][a]
P1	77.1	130.5	1.69	90	310
P2	10.6	13.4	1.26	142	305
P3	175.0	318.0	1.82	133	400
APFO-3	6.2	14.0	2.26	90	365

[a] Degradation temperature was calculated from the onset temperature of decomposition of polymer.

connected to a Water 410 differential refractometer with THF as an eluent. Electronic absorption spectra were obtained on a SHIMADZU UV-visible spectrometer model UV-1601PC. Fluorescence spectra were recorded on a Varian FLR025. Elemental analyses were performed on a Flash EA 1112 analyzer. TGA (Pyris 1 TGA) measurements were carried out under a nitrogen atmosphere at a heating rate of 10 °C/min to record the thermal gravimetric analysis (TGA). Atomic force microscopy (AFM) measurements were performed under ambient conditions using a Digital Instrument Multimode Nanoscope IIIA operating in the tapping mode. The highest occupied molecular orbital (HOMO) levels of all molecules synthesized in this study were determined by ultraviolet photoelectron spectroscopy (UPS) measurements of a bulk thin film spin-coated on ITO. UPS characterizations (binding energy error of about 100 meV) were carried out with monochromatized *HeI* radiation at 21.2 eV in ultra high vacuum. HOMO values are here defined as the vertical ionization potential derived from UPS.

2.2. Fabrication and characterization of polymer solar cells

OSCs were fabricated with the device configuration of ITO/PEDOT:PSS/active layer/LiF/Al. The conductivity of ITO was 20 Ω/□ and PEDOT:PSS is Baytron AI 4083 from H. C. Starck. A thin layer of PEDOT:PSS was spin coated on top of cleaned ITO substrate at 3000 rpm/s and dried subsequently at 120 °C for 10 min on a hotplate before transferred into a glove box. The active layer was prepared by spin-coating the chloroform or dichlorobenzene solution of polymers and $PC_{71}BM$ on the top of ITO/PEDOT:PSS. The top electrode was thermally evaporated, with a 0.6 nm LiF layer, followed by 80 nm of aluminum at a pressure of 10^{-6} Torr through a shadow mask. The configurations of the solar cells are the same as in ref 16. Four OSCs were fabricated on one substrate and the effective area of one cell is between 4 mm^2 and 6 mm^2. Current-voltage characteristics were recorded using a Keithley 2400 Source Meter under AM 1.5 illumination with an intensity of 100 mW cm^{-2} from a solar simulator (Model SS-50A, photo Emission Tech., Inc.).

2.3. Field-effect transistors (FETs)

FETs are made from thermally oxidized highly doped p-type silicon wafers with an oxide thickness of 100 nm. Gold electrodes, with a chromium buffer layer, are thermally evaporated and patterned by lithography. Channel lengths (L) are in the range 10 and 50 μm and widths (W) around 5 mm. The active layer is spin coated on top. Evaluation of the FET data is done in the saturated regime from derivative plots of the square root of the source-drain current versus gate voltage. Where hysteresis or other effects prevents a constant slope, the maximum slope for outgoing (off to on) sweeps was used. Measurements were done under high vacuum ($\sim 10^{-6}$ torr).

2.4. Synthesis of polymers

2.4.1. General procedures for the preparation of polymer *P1*, *P2* and *P3*

A mixture of monomers, THF or THF/Toluene, water, $NaHCO_3$ and the catalyst precursor $Pd(PPh_3)_4$ was carefully degassed and charged with nitrogen. The reaction mixture was stirred and refluxed for 3 days. Phenyl boronic acid and bromobenzene were used successively to end-cap the polymer after polymerization. $CHCl_3$ was then added; the organic layer was separated and dried over Na_2SO_4. After the removal of most solvent, the residue was

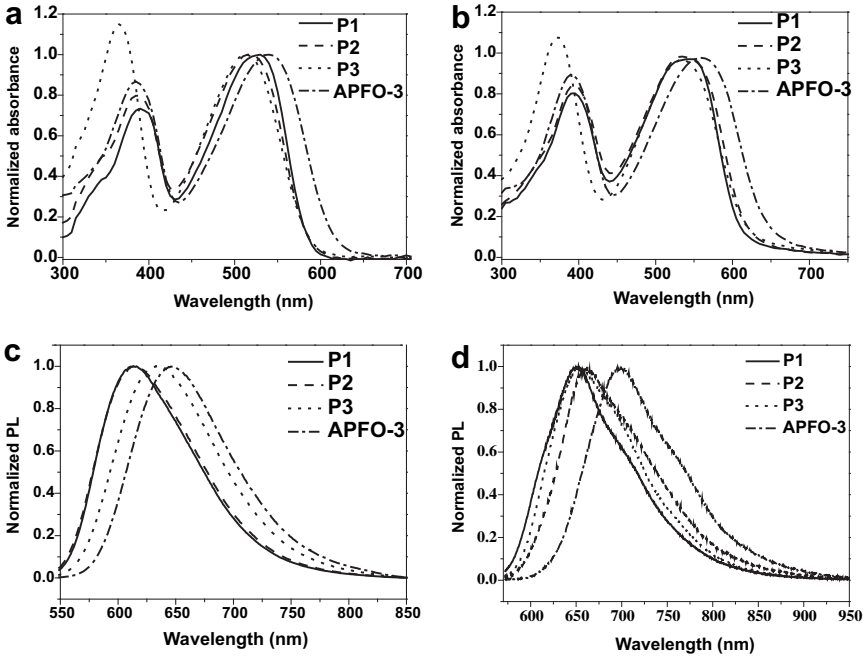

Fig. 1. Normalized absorption spectra of **P1**–**3** and **APFO-3** (a) in THF solution and (b) in thin films; Normalized photoluminescence spectra of **P1**–**3** and **APFO-3** (c) in THF solution and (d) in thin films.

Table 2
Summary of absorption, emission, optical bandgap and HOMO Level of **P1**–**3** and **APFO-3**.

Polymers	Absorption λ_{max} (nm) in THF	Absorption λ_{max} (nm) in film	Emission λ_{max} (nm) in THF[a]	Band gap[b]	HOMO[c] ± 0.1 (eV)
P1	530	550	650	2.01	−5.5
P2	520	535	660	1.96	−5.4
P3	510	535	655	1.97	−5.6
APFO-3	540	560	700	1.86	−5.5

[a] Polymer films were excited at 540 nm.
[b] Band gaps were calculated from the onset value of absorption in films.
[c] HOMO levels were measured by UPS.

poured into a large amount of acetone and the resulted precipitates were collected by filtration. The crude product was subjected to Soxhlet extraction with acetone for 2 days, dissolved in a minimum amount of $CHCl_3$, and precipitated into a large amount of acetone. The formed dark precipitates were collected by filtration and dried in high vacuum.

2.4.2. Synthesis of *P1*

4 (0.11 g, 0.16 mmol), **5** (0.1 g, 0.16 mmol), THF (15 mL), Toluene (5 mL), H_2O (3 mL), $NaHCO_3$ (0.2 g, 2.4 mmol) and $Pd(PPh_3)_4$ (1.8 mg, 1.6 μmol) were used. 104 mg (a yield of 69%) of **P1** was obtained. ^{1}H NMR (400 MHz, $CDCl_3$) δ 8.59 (m, 2H), 7.73-7.77 (broad, 6H), 7.27 (m, 2H), 4.25 (m, 4H), 2.07 (m, 8H), 1.58 (m, 4H), 1.34-1.41 (broad, 16H), 1.13-1.20 (broad, 20H), 0.79-0.92 (broad, 12H). ^{13}C NMR (100 MHz, $CDCl_3$) δ 152.05, 151.23, 146.63, 140.70, 133.72, 133.58, 132.23, 125.15, 123.19, 120.39, 120.29, 117.77, 74.76, 55.59, 40.77, 32.09, 32.00, 30.82, 30.32, 29.90, 29.59, 29.48, 26.37, 24.10, 22.91, 22.80, 14.33, 14.25. Anal. Calcd. for $[C_{59}H_{78}N_2O_2S_3]_n$: C, 75.11; H, 8.33; N, 2.97. Found: C, 73.76; H, 8.25; N, 4.23.

2.4.3. Synthesis of *P2*

4 (0.4 g, 0.56 mmol), **6** (0.25 g, 0.56 mmol), THF (10 mL), Toluene (30 mL), H_2O (6 mL), $NaHCO_3$ (0.71 g, 8.4 mmol) and $Pd(PPh_3)_4$ (6.5 mg, 5.6 μmol) were used. 358 mg (a yield of 86%) of **P2** was obtained. ^{1}H NMR (400 MHz, $CDCl_3$) δ 8.50 (m, 2H), 7.75 (m, 6H), 7.42 (m, 2H), 4.23 (m, 4H), 2.04 (m, 4H), 1.64-1.31 (broad, 26H), 0.89 (m, 6H). ^{13}C NMR (100 MHz, $CDCl_3$) δ 155.50, 155.47, 152.66, 151.83, 147.00, 139.34, 134.51, 134.47, 134.43, 132.85, 126.01, 125.98, 123.88, 123.87, 123.85, 123.82, 121.42, 121.38, 121.34, 120.84, 120.82, 118.36, 75.35, 47.93, 32.76, 31.47, 30.57, 30.53, 30.23, 30.17, 28.21, 28.16, 28.11, 27.04, 23.59, 23.56, 14.99, 1.89, 0.86. Anal. Calcd. for $[C_{45}H_{50}N_2O_2S_3]_n$: C, 72.35; H, 6.75; N, 3.75. Found: C, 69.92; H, 7.36; N, 3.68.

2.4.4. Synthesis of *P3*

7 (0.63 g, 1 mmol), **5** (0.64 g, 1 mmol), THF (30 mL), H_2O (6 mL), $NaHCO_3$ (1.26 g, 15 mmol) and $Pd(PPh_3)_4$ (11.6 mg, 10 μmol) were used. 0.59 g (a yield of 69%) of **P3** was obtained. ^{1}H NMR (400 MHz, $CDCl_3$) δ 8.08 (m, 2 H), 7.90 (m, 2H), 7.80 (m, 2H), 7.53 (m, 4H), 2.82 (m, 4H), 2.0 (m, 10 H), 1.70–1.10 (broad, 37H), 0.90–0.80 (broad, 9H). ^{13}C NMR (100 MHz, $CDCl_3$) δ 152.71, 151.30, 140.34, 140.17, 139.86, 130.43, 128.21, 125.73, 125.27, 123.57, 119.91, 55.27, 31.80, 31.73, 31.12, 30.15, 29.35, 29.31, 24.00, 22.65, 22.61, 14.08. Anal. Calcd. for $[C_{55}H_{70}N_2S_3]_n$: C, 77.23; H, 8.25; N, 3.28. Found: C, 76.64; H, 8.23; N, 3.30.

3. Results and discussion

3.1. Synthesis and characterization of polymers

The syntheses of conjugated polymers **P1**–**3** are outlined in Scheme 1. All polymers are prepared by Suzuki-Miyaura-Schlüter Polycondensation (SMSPC). **P1** was synthesized in a yield of 69% by SMSPC of 4,7-bis(5-bromothiophen-2-yl)-5,6-bis(octyloxy) -2,1,3-benzothiadiazole (**4**) and 4,4,5,5-tetramethyl-2-(2-(4,4,5, 5-tetramethyl-1,3,2- dioxaborolan-2-yl)-9,9-dioctyl-9H-fluoren-7-yl)-1,3,2-dioxaborolane (**5**) with $Pd(PPh_3)_4$ as the catalyst precursor and tetrahydrofuran (THF)/toluene/H_2O as the reaction media. Similarly, **P2** was synthesized in a yield of 86% by SMSPC of monomer **4** and 4,4,5,5-tetramethyl-2-(9,9-dimethyl-2-(4,4,5,5-tetramethyl-1,3,2-dioxaborolan-2-yl)-9H-fluoren-7-yl)-1,3,2-dioxaborolane (**6**). **P3** was synthesized in a yield of 69% by SMSPC of 4,7-bis(5-bromo-4-hexylthiophen-2-yl)-2,1,3-benzothiadiazole (**7**) and monomer **5** with $Pd(PPh_3)_4$ as the catalyst precursor and THF/H_2O as the reaction media. THF/toluene/aqueous $NaHCO_3$ solution was used as the reaction medium for the preparation of **P1** and **P2**, since these two polymers precipitate in the THF/aqueous $NaHCO_3$ solution during polymerization [51]. The structure and photovoltaic properties of **P3** have been previously published in the literature [52]. **APFO-3** was synthesized by following literature procedure [39]. The structures of these polymers were confirmed by ^{1}H and ^{13}C NMR spectroscopy. Molecular weights of these polymers were measured by GPC calibrated with polystyrene standards with THF as an eluent. The data are summarized in Table 1. Considerably high molecular weights have been achieved for **P1** and **P3**. The relatively low molecular weight for polymer **P2** and **APFO-3** is probably due to the poor solubility of these two polymers in the organic solvent(s) used in the polycondensation. They precipitated from the reaction media during the polycondensation. Fortunately, the precipitated polymers are readily soluble in chloroform and 1,2-dichlorobenzene (DCB). All polymers exhibit good solubility in chloroform and DCB. Thermogravimetric analysis (TGA) indicated that **P1** and **P2** with two octyloxy chains on the benzothiadiazole unit have lower decomposition temperatures than **P3** and **APFO-3** based on unsubstituted benzothiadiazole. The data are summarized in Table 1. Glass transition temperatures (T_g) of the four polymers are also listed in Table 1, among which **P1** and **APFO-3** demonstrated lower T_g of 90 °C.

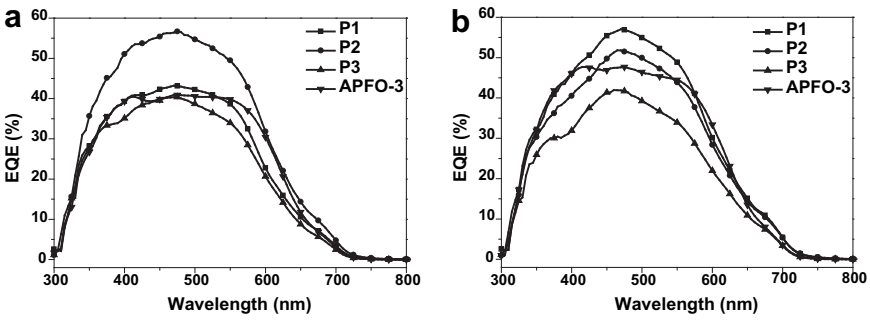

Fig. 2. EQE of bulk heterojunction OSCs based on polymers and $PC_{71}BM$ spin-coated from solvent a) chloroform and b) DCB.

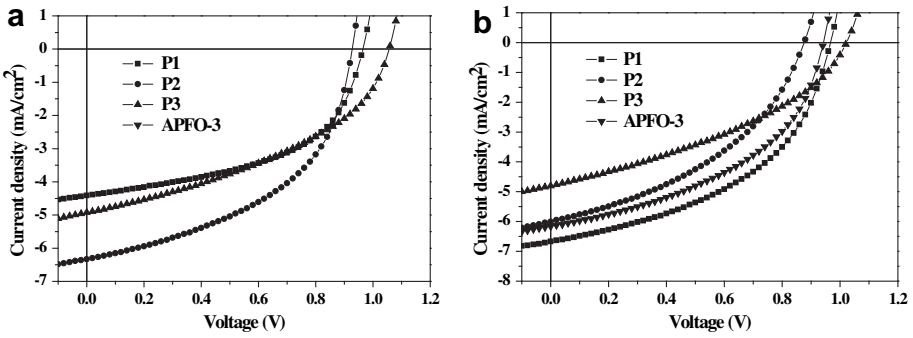

Fig. 3. Current–voltage characteristics of OSCs based on polymers and $PC_{71}BM$ spin-coated from solvent a) chloroform and b) DCB.

3.2. Optical properties

Normalized absorption spectra of polymers **P1**–**3** and **APFO-3** in THF solution and films are shown in Fig. 1(a) and (b), respectively. All polymers show two broad absorption bands in the range of 300–430 nm and 450–700 nm. Compared with **APFO-3**, the absorption peaks of **P1**–**3** are blue-shifted both in solution and films. **P1** and **P2** show the similar absorption spectra, which indicate that the length of alkyl substituents on 9-position of the fluorene unit has a weak influence on the conjugation of polymer main chain. Compared with **APFO-3**, the absorption peak of **P3** in THF solution is markedly blue-shifted due to the steric hinderance of hexyl chains in the 4-position of the thiophene [41,42]. Optical band gaps for **P1**–**3** also increased in comparison with **APFO-3**. The optical properties of polymers and HOMO level measured by UPS are summarized in Table 2. For the four polymers, the HOMO levels are not greatly varied.

Normalized photoluminescence (PL) spectra of these polymers in THF solution and thin films excited at 540 nm are shown in Fig. 1(c) and (d), respectively. In solution and in films, all polymers emit red-light. In solution, the normalized emission spectra of **P1** and **P2** are almost superimposed; whereas in films, the emission peak of **P2** is slightly red-shifted in comparison with that of **P1**. This is probably due to that the two longer octyl groups on the 9-position of fluorene in **P1** can more effectively suppress the aggregation of the polymer backbone than that of the two methyl groups in **P2**. For all polymers, in the blend films of polymer: $PC_{71}BM$, there is no detectable emission of polymers when high fullerene content (1:3, wt%) was used, indicating efficient exciton dissociation in the blends, which effectively quench the fluorescence of polymers.

3.3. Photovoltaic properties

Photovoltaic properties of these polymers were investigated in devices with the structure of ITO/PEDOT:PSS/active layer/LiF/Al. The active layer is a blend of **P1**, **P2**, **P3** or **APFO-3** donor and $PC_{71}BM$ acceptor. Solar cells were fabricated from chloroform or DCB solution. The ratio of donor to acceptor and the thickness were optimized. Optimum performance was always achieved with a ratio of polymer to $PC_{71}BM$ of 1:3 (w/w) and an active layer thickness in the range of 70 nm to 90 nm.

Table 3
Characteristic properties of polymers/$PC_{71}BM$ solar cells.

Active layer	Solvent	Thickness [nm]	J_{sc} [mA/cm^2]	V_{oc} [V]	FF	PCE [%]
P1/$PC_{71}BM$	Chloroform	85	4.4	0.96	0.52	2.2
P1/$PC_{71}BM$	DCB	80	6.7	0.97	0.47	3.1
P2/$PC_{71}BM$	Chloroform	80	6.3	0.93	0.48	2.8
P2/$PC_{71}BM$	DCB	85	6.0	0.88	0.42	2.2
P3/$PC_{71}BM$	Chloroform	80	4.9	1.06	0.41	2.2
P3/$PC_{71}BM$	DCB	75	4.8	1.02	0.38	1.9
APFO-3/$PC_{71}BM$	Chloroform	70	4.5	0.98	0.46	2.0
APFO-3/$PC_{71}BM$	DCB	70	6.2	0.94	0.46	2.7

External quantum efficiencies (EQEs) of OSCs based on blend films of polymer and $PC_{71}BM$ spin-coated from chloroform and DCB under monochromatic illumination are shown in Fig. 2(a) and (b). Polymer **P1** has a higher EQE with the peak at 57% from DCB solution, which is higher than that obtained from chloroform solution (43%). A similar phenomenon was also found for **APFO-3**, in which the EQE peak is 48% from DCB solution and 41% from chloroform. Polymer **P2** and **P3** based OSCs show high EQE from chloroform solution, in which the EQE peaks are 57% for **P2** and 41% for **P3**. The large variations of EQE performance from different solutions should be due to the influence of flexible side chains of conjugated polymers and hence the distinct morphology, which will be discussed vide infra.

The *I*–*V* characteristics of OSCs were recorded under simulated solar illumination of AM 1.5 G with an incident power density of 100 mW/cm^2 and are shown in Fig. 3. The parameters of the OSCs are also summarized in Table 3. Devices based on polymer **P1** and **APFO-3** displayed higher J_{sc} and PCE from DCB solution, with $J_{sc} = 6.7$ mA/cm^2, PCE 3.1% for **P1** and $J_{sc} = 6.2$ mA/cm^2, PCE 2.7% for **APFO-3**. Adversely, **P2** and **P3** show higher J_{sc} and PCE from chloroform solution, with $J_{sc} = 6.3$ mA/cm^2, PCE 2.8% for **P2** and $J_{sc} = 4.9$ mA/cm^2, PCE 2.2% for **P3**. By comparing the performance of **P1** and **APFO-3** based OSCs, it obviously shows that J_{sc}, FF and PCE of **P1** are comparable with that of **APFO-3**, which means that the introduction of octyloxy substituents to benzothiadiazole has little influence on the absorbance and carrier transport property of the conjugated polymer main chain. However, the device performance of **P3** with hexyl substituents on thiophene moiety was decreased, suggesting a negative effect on photovoltaic performance when introducing alkyl chains on the thiophene units. Our results show that the introduction of flexible side chains on the benzothiadiazole unit is a successful approach to increase solubility and molecular weight of conjugated polymers, while still keeping the performance of devices comparable to that of corresponding polymers with unsubstituted benzothiadiazole units.

To explain the performance difference of devices from two solvents, chloroform and DCB, atomic force microscopy (AFM) was used to investigate the morphology of blend films. Height images of blend films spin-coated from chloroform and DCB solutions are shown in Fig. 4 and root mean square (RMS) values are summarized below images. Blend films of **P1**/$PC_{71}BM$ and **APFO-3**/$PC_{71}BM$ spin-coated from chloroform solution exhibited a large scale phase separation (about 200 nm domains) and relatively high RMS values,

which are not favorable for the charge separation and hence end up with lower current densities. On the contrary, blend films of **P2** and **P3** from chloroform solution have a fairly small phase separation, resulting in higher current densities.

3.4. Mobility measurements

To further investigate the relationship between solvents and device performances, mobilities of pure polymers and polymer:

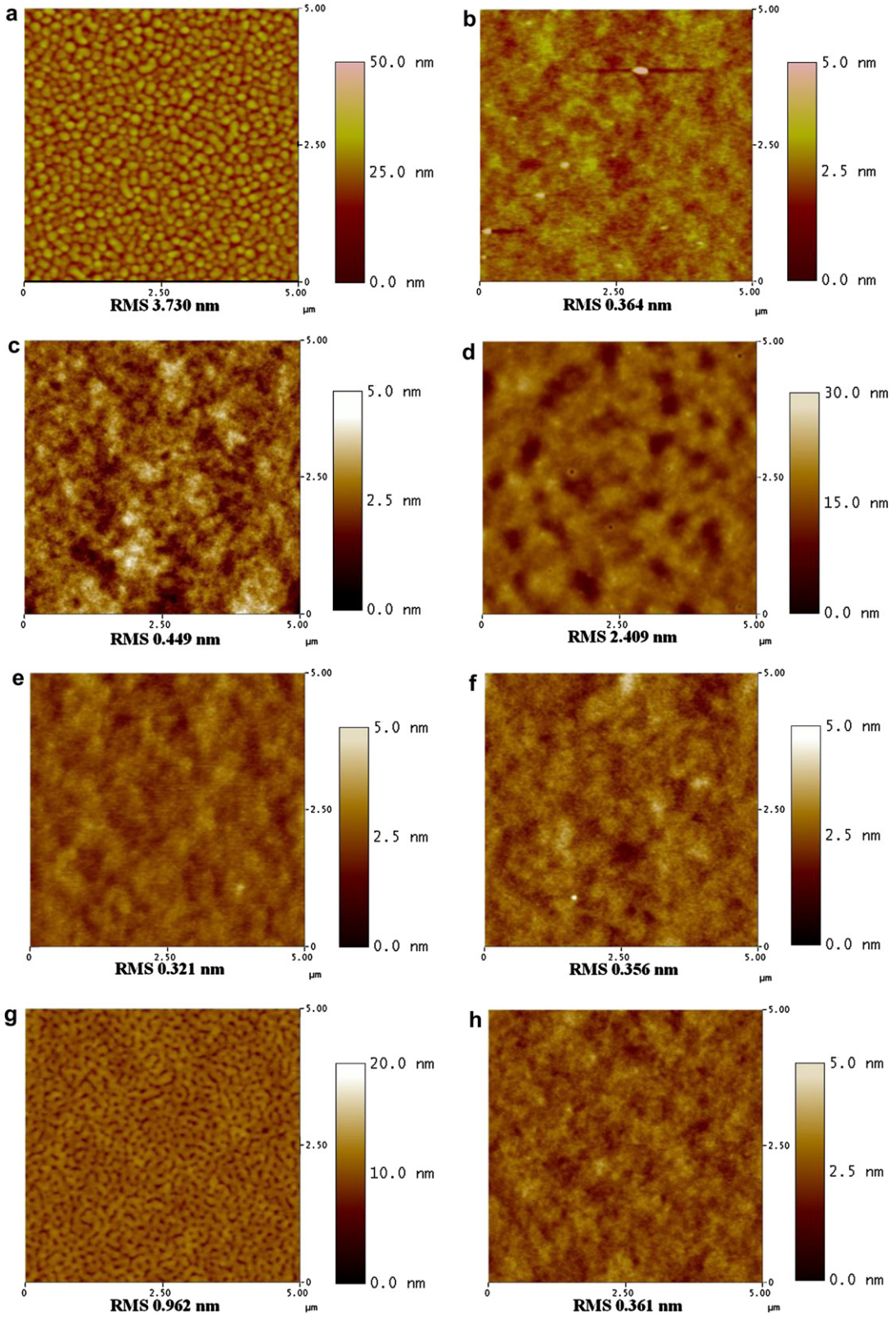

Fig. 4. AFM height images of blend films spin-coated from chloroform solution a) **P1**/$PC_{71}BM$ c) **P2**/$PC_{71}BM$ e) **P3**/$PC_{71}BM$ and g) **APFO-3**/$PC_{71}BM$; from DCB solution b) **P1**/$PC_{71}BM$ d) **P2**/$PC_{71}BM$ f) **P3**/$PC_{71}BM$ and h) **APFO-3**/$PC_{71}BM$. RMS values are also listed below the figures.

Table 4
Average field effect transistor mobilities of pure polymers and the blends used for optimized solar cells. The standard deviations of the mobilities are given in parenthesis.

	Pure polymer	Blend film from Chloroform		Blend film from DCB	
	Hole mobility [$cm^2 Vs^{-1}$]	Hole mobility [$cm^2 Vs^{-1}$]	Electron mobility [$cm^2 Vs^{-1}$]	Hole mobility [$cm^2 Vs^{-1}$]	Electron mobility [$cm^2 Vs^{-1}$]
P1	2×10^{-5} (8×10^{-6})	1×10^{-2} (3×10^{-3})	1×10^{-3} (8×10^{-5})	6×10^{-4} (4×10^{-4})	8×10^{-4} (5×10^{-4})
P2	1×10^{-4} (6×10^{-5})	4×10^{-4} (2×10^{-4})	9×10^{-4} (4×10^{-4})	8×10^{-5} (3×10^{-6})	6×10^{-4} (6×10^{-5})
P3	Very low	1×10^{-3} (8×10^{-4})	5×10^{-4} (4×10^{-4})	1×10^{-3} (2×10^{-4})	4×10^{-3} (2×10^{-4})
APFO-3	1×10^{-4} (1×10^{-5})	4×10^{-3} (2×10^{-3})	4×10^{-4} (2×10^{-4})	3×10^{-4} (8×10^{-5})	4×10^{-4} (2×10^{-5})

$PC_{71}BM$ blends spin-coated from chloroform or DCB solutions were studied by field effect transistors, and the results are presented in Table 4. All values are based on the maximum slope of the square root of the transfer characteristics of the devices. This slope is fairly constant for some of materials and mobilities but varies strongly for others, and it should be noted that especially in those cases are unusually high mobilities obtained, such as for the hole mobility of **P1** from chloroform solution, the variation in mobility with gate voltage is very large. All data are collected from four devices with different geometries on the same substrate.

All pure polymers exhibit lower hole mobilities than their respective blends. Most notably, the hole mobility of pure polymer **P3** is too low to be accurately determined with the same sample geometries used for the other materials, and although mobilities of blend films, especially from chloroform solution, are quite good, the OSC performance indicates poor transport, consistently with the measurement on the pure material. Where the morphology and short circuit currents are comparable (**P1**, **APFO-3** with $PC_{71}BM$ from DCB, and **P2**, **P3** with $PC_{71}BM$ from chloroform), it always shows balanced hole and electron mobility. It is also interesting to note that in two cases (**P1**/$PC_{71}BM$ and **APFO-3**/$PC_{71}BM$) where chloroform solutions give large domains, hole mobilities are unusually high, but electron mobilities and PCEs are relatively low.

4. Conclusions

In conclusion, a series of conjugated polymers **P1**–**3** carrying flexible side chains at different positions of conjugated main chains were synthesized by SMSPC and compared with polymer **APFO-3**. High molecular weight polymers **P1** and **P3**, which bear four flexible alkyl chains at each repeat unit, were obtained. Photovoltaic devices based on polymer/$PC_{71}BM$ blend films spin-coated from chloroform or DCB solution were investigated. The morphology of blend films, which influences the performance of photovoltaic cells, was dependent on solvent. **P1**, with two octyloxy chains on benzothiadiazole and two octyl chains on fluorene, shows the best performance among these polymers, with a PCE of 3.1%. Our results show that the modification of the benzothiadiazole with two octyloxy chains can greatly increase molecular weights and processibility while retaining a high PCE.

Acknowledgments

The work was conducted through the collaboration between Linköping University, Sweden, and Institute of Chemistry, Chinese Academy of Sciences, financed by Swedish Research Links Program of Swedish Research Council (VR). Financial support by the NSF of China (50603027, 20834006 and 50821062) and the 863 Program (2008AA05Z425) is gratefully acknowledged. We thank Professor M. R. Andersson at Chalmers University for supplying **APFO-3** and Prof. Olle Inganäs of Linköping University for providing the facility to conduct the research.

Appendix. Supporting information

^{1}H-NMR spectra, ^{13}C-NMR spectra, DSC of polymers. This material is available free of charge via the internet at doi:10.1016/j.polymer.2010.05.015.

References

[1] Krebs FC. Solar Energy Materials and Solar Cells 2009;93(4):394.
[2] Dennler G, Scharber MC, Brabec CJ. Advanced Materials 2009;21(13):1323.
[3] Li G, Shrotriya V, Huang JS, Yao Y, Moriarty T, Emery K, et al. Nature Materials 2005;4(11):864.
[4] Ma WL, Yang CY, Gong X, Lee K, Heeger AJ. Advanced Functional Materials 2005;15(10):1617.
[5] Liang YY, Feng DQ, Wu Y, Tsai ST, Li G, Ray C, et al. Journal of the American Chemical Society 2009;131(22):7792.
[6] Park SH, Roy A, Beaupré S, Cho S, Coates N, Moon JS, et al. Nature Photonics 2009;3(5):297.
[7] Wang EG, Wang L, Lan LF, Luo C, Zhuang WL, Peng JB, et al. Applied Physics Letters 2008;92(3):033307.
[8] Peet J, Kim JY, Coates NE, Ma WL, Moses D, Heeger AJ, et al. Nature Materials 2007;6(7):497.
[9] Qin RP, Li WW, Li CH, Du C, Veit C, Schleiermacher HF, et al. Journal of the American Chemical Society 2009;131(41):14612.
[10] Hou JH, Chen HY, Zhang SQ, Li G, Yang Y. Journal of the American Chemical Society 2008;130(48):16144.
[11] Hou JH, Chen HY, Zhang SQ, Chen RI, Yang Y, Wu Y, et al. Journal of the American Chemical Society 2009;131(43):15586.
[12] Bundgaard E, Krebs FC. Solar Energy Materials and Solar Cells 2007;91(11):954.
[13] Inganäs O, Zhang FL, Andersson MR. Accounts of Chemical Research 2009;42(11):1731.
[14] Li YF, Zou YP. Advanced Materials 2008;20(15):2952.
[15] Roquet S, Cravino A, Leriche P, Alévêque O, Frère P, Roncali J. Journal of the American Chemical Society 2006;128(10):3459.
[16] Svensson M, Zhang FL, Veenstra SC, Verhees WJH, Hummelen JC, Kroon JM, et al. Advanced Materials 2003;15(12):988.
[17] Kitazawa D, Watanabe N, Yamamoto S, Tsukamoto J. Applied Physics Letters 2009;95(8):053701.
[18] Chen MH, Hou JH, Hong ZR, Yang GW, Sista S, Chen LM, et al. Advanced Materials 2009;21(42):4238.
[19] Lindgren LJ, Zhang FL, Andersson M, Barrau S, Hellstrom S, Mammo W, et al. Chemistry of Materials 2009;21(15):3491.
[20] Li YF, Li H, Xu B, Li ZF, Chen FP, Feng DQ, et al. Polymer 2010;51:1786.
[21] Blouin N, Michaud A, Leclerc M. Advanced Materials 2007;19(17):2295.
[22] Zou YP, Gendron D, Badrou-Aich R, Najari A, Tao Y, Leclerc M. Macromolecules 2009;42(8):2891.
[23] Boudreault PLT, Michaud A, Leclerc M. Macromolecular Rapid Communications 2007;28(22):2176.
[24] Muhlbacher D, Scharber M, Morana M, Zhu ZG, Waller D, Gaudiana R, et al. Advanced Materials 2006;18(22):2931.
[25] Li KC, Hsu YC, Lin JT, Yang CC, Wei KH, Lin HC. Journal of Polymer Science Part A-Polymer Chemistry 2009;47(8):2073.
[26] Moule AJ, Tsami A, Buennagel TW, Forster M, Kronenberg NM, Scharber M, et al. Chemistry of Materials 2008;20(12):4045.
[27] Zhou EJ, Nakamura M, Nishizawa T, Zhang Y, Wei QS, Tajima K, et al. Macromolecules 2008;41(22):8302.
[28] Zhou EJ, Yamakawa S, Tajima K, Yang CH, Hashimoto K. Chemistry of Materials 2009;21(17):4055.
[29] Liao L, Dai LM, Smith A, Durstock M, Lu JP, Ding JF, et al. Macromolecules 2007;40(26):9406.
[30] Kim J, Park SH, Cho S, Jin Y, Kim J, Kim I, et al. Polymer 2010;51(2):390.
[31] Zhang FL, Bijleveld J, Perzon E, Tvingstedt K, Barrau S, Inganäs O, et al. Journal of Materials Chemistry 2008;18(45):5468.
[32] Yi HN, Johnson RG, Iraqi A, Mohamad D, Royce R, Lidzey DG. Macromolecular Rapid Communications 2008;29(22):1804.
[33] Tamayo AB, Dang XD, Walker B, Seo J, Kent T, Nguyen TQ. Applied Physics Letters 2009;94(10):103301.

[34] Wienk MM, Turbiez M, Gilot J, Janssen RAJ. Advanced Materials 2008;20(13):2556.
[35] Zoombelt AP, Gilot J, Wienk MA, Janssen RAJ. Chemistry of Materials 2009;21(8):1663.
[36] Petersen MH, Hagemann O, Nielsen KT, Jorgensen M, Krebs FC. Solar Energy Materials and Solar Cells 2007;91(11):996.
[37] Palmaerts A, Lutsen L, Cleij TJ, Vanderzande D, Pivrikas A, Neugebauer H, et al. Polymer 2009;50(21):5007.
[38] Nguyen LH, Hoppe H, Erb T, Gunes S, Gobsch G, Sariciftci NS. Advanced Functional Materials 2007;17(7):1071.
[39] Inganäs O, Svensson M, Zhang F, Gadisa A, Persson NK, Wang X, et al. Applied Physics A-Materials Science & Processing 2004;79(1):31.
[40] Wang EG, Wang M, Wang L, Duan CH, Zhang J, Cai WZ, et al. Macromolecules 2009;42(13):4410.
[41] Jayakannan M, Van Hal PA, Janssen RAJ. Journal of Polymer Science Part A-Polymer Chemistry 2002;40(14):2360.
[42] Jayakannan M, Van Hal PA, Janssen RAJ. Journal of Polymer Science Part A-Polymer Chemistry 2002;40(2):251.
[43] Zoombelt AP, Leenen MAM, Fonrodona M, Nicolas Y, Wienk MM, Janssen RAJ. Polymer 2009;50(19):4564.
[44] Ma W, Kim JY, Lee K, Heeger AJ. Macromolecular Rapid Communications 2007;28(17):1776.
[45] Koppe M, Brabec CJ, Heiml S, Schausberger A, Duffy W, Heeney M, et al. Macromolecules 2009;42(13):4661.
[46] Schilinsky P, Asawapirom U, Scherf U, Biele M, Brabec CJ. Chemistry of Materials 2005;17(8):2175.
[47] Hiorns RC, De Bettignies R, Leroy J, Bailly S, Firon M, Sentein C, et al. Advanced Functional Materials 2006;16(17):2263.
[48] Ballantyne AM, Chen L, Dane J, Hammant T, Braun FM, Heeney M, et al. Advanced Functional Materials 2008;18(16):2373.
[49] Guntner R, Farrell T, Scherf U, Miteva T, Yasuda A, Nelles G. Journal of Materials Chemistry 2004;14(17):2622.
[50] Coulson DR. Inorganic Syntheses 1972;13:121.
[51] Sun MH, Li J, Li BS, Fu YQ, Bo ZS. Macromolecules 2005;38(7):2651.
[52] McNeill CR, Abrusci A, Zaumseil J, Wilson R, McKiernan MJ, Burroughes JH, et al. Applied Physics Letters 2007;90(19):193506.